Canadian Journal of Fisheries and Aquatic Sciences

OPEN ACCESS | Research Article

Widespread high prevalence of vaterite in Pink Salmon (*Oncorhynchus gorbuscha*) otoliths

Frode Pedersen[a,b], **Henrik H. Berntsen**[b], **Eva B. Thorstad**[b], **Michał E. Skóra**[c,d], **J. Iwan Jones**[c], **Gareth D. Davies**[e], **Sigurd Einum**[a], **Kirstin Eliasen**[f], **Guðni Guðbergsson**[g], **Narve Stubbraaten Johansen**[b], **Michael Millane**[h], **Julius Nielsen**[i], **Edward O. Otis**[j], **Dion S. Oxman**[k], **Sean Robertson**[l], **Jamie Urquhart**[m], **Kjell R. Utne**[n], **and Malte Willmes**[b,o]

[a]Norwegian University of Science and Technology, Faculty of Natural Sciences, Department of Biology, Trondheim, Norway; [b]Norwegian Institute for Nature Research, PO Box 5685, 7485 Torgarden, Trondheim, Norway; [c]School of Biological and Behavioural Sciences, Queen Mary University of London, London, UK; [d]University of Gdańsk, Faculty of Oceanography and Geography, Professor Krzysztof Skóra Hel Marine Station, Hel, Poland; [e]Environment Agency, UK; [f]Firum, Við Áir 11, 430 Hvalvík, Faroe Islands; [g]Marine and Freshwater Research Institute, Hafnarfjörður, Iceland; [h]Inland Fisheries Ireland, Dublin, Ireland; [i]Greenland Institute of Natural Resources, Nuuk, Greenland; [j]Alaska Department of Fish and Game, 3298 Douglas Place, Homer, AK 99603, USA; [k]Alaska Department of Fish and Game, Juneau, AK, USA; [l]Fisheries Management Scotland, Edinburgh, UK; [m]Dee District Salmon Fishery Board & River Dee Trust, UK; [n]Institute of Marine Research, Bergen, Norway; [o]Institute of Marine Sciences, University of California Santa Cruz, Santa Cruz, CA, USA

Corresponding author: **Frode Pedersen** (email: frode.pedersen@nina.no)

Abstract

Pacific salmonids rely on precise sensory mechanisms, including the sagittal otolith, to support long-distance migrations. Vaterite replacement of otolith aragonite can impair sensory function, and compromise otolith-based reconstructions of environmental history. Otoliths from 1116 native and invasive Pink Salmon across the Pacific and Atlantic Oceans were examined for vaterite prevalence, coverage, and timing of formation. Visual assessment proved to be a reliable and efficient method for identifying otolith mineralogy, based on validation using X-ray diffraction ($R^2 = 0.99$, $p < 0.001$). We document exceptionally high vaterite prevalence in Pink Salmon from both Atlantic (97%) and Pacific (94%–96%) populations, with minimal geographic variation and no differences among native and invasive or wild and hatchery populations. Mean vaterite coverage within otolith pairs was 49 ± 27% ($n = 449$). The prevalence of vaterite far exceeded that reported for other salmonids, including hatchery-reared populations. Our results indicate that vaterite formation can occur at any life stage, beginning as early as the juvenile freshwater stage and peaking early in the marine phase. Overall, our findings support an association between the unusually high prevalence of vaterite in Pink Salmon and a life-history strategy characterized by rapid growth.

Key words: invasive species, otoliths, Pink Salmon, vaterite, X-ray diffraction

Introduction

The Pink Salmon (*Oncorhynchus gorbuscha* (Walbaum, 1792)) is an anadromous fish species native to the northern Pacific Ocean. It is the most abundant Pacific salmon (*Oncorhynchus* spp.), comprising approximately 70% of total Pacific salmon abundance in the native range from 2005 to 2021 (Ruggerone et al. 2023). Typically, Pink Salmon have a 2-year life cycle, with adults returning to freshwater to spawn after 1 year at sea (Heard 1991), resulting in reproductively isolated even- and odd-year cohorts (Tarpey et al. 2018). Pink Salmon exert substantial ecological influence in native ecosystems: they provide critical food and nutrient subsidies to a wide array of species, from freshwater and riparian consumers to marine mammals and seabirds and support entire food webs through marine-derived nutrient cycling and biomass transfer (Brandt et al. 2024).

Pink Salmon are currently expanding their range within the Arctic Ocean beyond their historical distribution (Dunmall et al. 2024) as well as into the North Atlantic/Arctic from the White Sea in north-east Russia, where they were deliberately introduced to improve salmon landings (Lennox et al. 2023). The history of their introduction into the White Sea tributaries begins in 1956, with stocking of alevins originating from the Sakhalin Island (Sandlund et al. 2019). Initial introduction attempts over many years proved unsuccessful. However, from 1985, eggs sourced from a more northerly population on Russia's Pacific coast, the River Ola, led to a breakthrough, and Pink Salmon subsequently established self-sustaining populations in north-western Russia. As a result, stocking activities ceased in 1999 (Gordeeva and Salmenkova 2011).

In 2017, Pink Salmon began appearing in large numbers across the North Atlantic, marking a clear shift from sporadic occurrence to invasive status in the region. By 2023, their abundance had increased markedly in odd years, particularly in northern Norway (Sandlund et al. 2019; Staveley et al. 2025; Thorstad et al. 2025), with successful reproduction documented as far south as Scotland and as far west as Iceland (Skóra et al. 2023, 2024). The rapid growth of Pink Salmon stocks in the North Atlantic raises concerns about their impact on native fish, ecosystems, and fisheries (VKM 2020; Lennox et al. 2023; Thorstad et al. 2024)

Understanding the biology and life history of invasive Pink Salmon is crucial for management, both in their native and non-native ranges (Dunmall et al. 2025). One approach to gain such insights involves studying otoliths, the small, calcified structures located in the inner ear of teleost fish. Otoliths (ear stones) are metabolically inert and grow continuously by incorporating calcium and other elements from ambient water and diet, making them valuable natural recorders of the fish's life history (Campana 1999; Doubleday et al. 2013). Their growth patterns can reveal important information about individual fish, such as age, growth rates, and environmental histories (Campana 1999) but also have practical applications in fisheries management. For instance, otoliths can be marked during early development by manipulating water temperature, creating distinct thermal rings that serve as permanent markers. These thermal marks function like barcodes, allowing for the identification of hatchery-reared fish (Volk et al. 1999).

Teleost fish possess three pairs of otoliths, sagittae, lapilli, and asterisci. Although this varies among taxa, in salmonids the sagitta (hereafter referred to simply as the otolith) is the largest and most frequently studied. Otoliths predominantly consist of the aragonite polymorph of calcium carbonate (Thomas et al. 2019). Under certain conditions, aragonite can be replaced by another polymorph, vaterite, leading to larger, asymmetrical, and less dense otoliths (Tomás and Geffen 2003; Oxman et al. 2007; Reimer et al. 2016). The difference in density between vaterite and aragonite has been found to decrease hearing sensitivity within other members of *Oncorhynchus* (Oxman et al. 2007). This, in turn, could impair key behaviors such as foraging, navigation, and predator avoidance, negatively impacting the fitness of affected fish (Reimer et al. 2016; Vignon and Aymes 2020; Austad et al. 2021). Additionally, vateritic otoliths exhibit altered structural and elemental composition, which can interfere with age, growth, and life history reconstructions based on otolith analysis (Tzeng et al. 2007; Lewis et al. 2022).

Vaterite has been reported in most salmonid species, though its prevalence varies across species and environments. Differences are possibly influenced by variation in environmental conditions, growth rates, and developmental factors in wild and hatchery settings (Reimer et al. 2016, 2017). Hatchery environments are typically designed to optimize growth, and factors such as diet, water temperature, and rearing densities may influence otolith mineralization (Strong et al. 1986; Payan et al. 2004; Oxman et al. 2007; Reimer et al. 2017). More recent studies indicate that alterations to rearing conditions, including alternating water flow and early-life enrichment, are associated with reduced vaterite prevalence in hatchery-reared coho salmon (Gaffney et al. 2025, 2026).

Detecting vaterite efficiently is essential for monitoring its prevalence and can be accomplished via a range of different methods (Wood et al. 2022). X-ray diffraction (XRD) is a reliable method for mineral identification (Bunaciu et al. 2015). However, this method is destructive when used for mineral phase quantification in otoliths, as it requires the otolith to be crushed, rendering it unusable for other analyses. In contrast, visual assessment based on otolith morphology offers a faster, more cost-effective alternative that preserves the otoliths for subsequent growth and environmental reconstruction analyses (Austad et al. 2021; Lewis et al. 2022; Gaffney et al. 2025). Overall, knowledge of vaterite occurrence in Pink Salmon otoliths is scarce, with limited data from Pacific populations and no data currently available for Atlantic populations. Comparative analysis of native (Pacific) and invasive (Atlantic) populations may offer new insights into the potential role of environmental factors in the development and prevalence of vaterite. The aims of this study were to (1) evaluate the accuracy of visual assessment compared with XRD confirmation, determining whether visual identification can reliably distinguish between aragonite and vaterite and serve as a practical tool for large-scale monitoring of vaterite in Pink Salmon otoliths; (2) investigate prevalence and coverage of vaterite in native and invasive Pink Salmon populations; and (3) identify the onset of vaterite formation to provide insights into the mechanisms driving its development.

Materials and methods

Ethics approval

No fish were sampled specifically for this study. Because the samples were collected from deceased fish that had been killed as part of other activities, ethics approval and research permits for the use of experimental animals were not required under Norwegian law. In the North Atlantic area, where the presence of non-native Pink Salmon poses a significant biological risk to native ecosystems (Forsgren et al. 2023) and their removal is encouraged, samples were collected from dead Pink Salmon caught as bycatch, by recreational anglers, or from targeted removal operations organized by the Norwegian government to limit further spread and establishment of invasive Pink Salmon (Thorstad et al. 2025). The organizations/persons performing targeted fishing for Pink Salmon with weirs or other catch methods had river-based licenses issued from County Governors or the Environment Agency in Norway, and commercial use of the Pink Salmon for human food consumption was based on requirements from the Norwegian Food Safety Authority. Samples from the Pacific were collected opportunistically from Pink Salmon caught in commercial fisheries permitted and licensed by the State of Alaska in the US.

Fig. 1. Map of the native range of Pink Salmon (blue) and introduced range (orange), according to ICES (2022); Skóra et al. (2023), (2024); Jensen et al. (2024); Nielsen et al. (2024); and Augerot (2005). Note that the distribution does not distinguish between occurrence or established and temporary spawning sites and does not differentiate between odd- and even-year populations. The background map was generated using the R package "rnaturalearth" (Massicotte and South 2023) and displayed in the WGS84 geographic coordinate system (latitude–longitude; EPSG:4326).

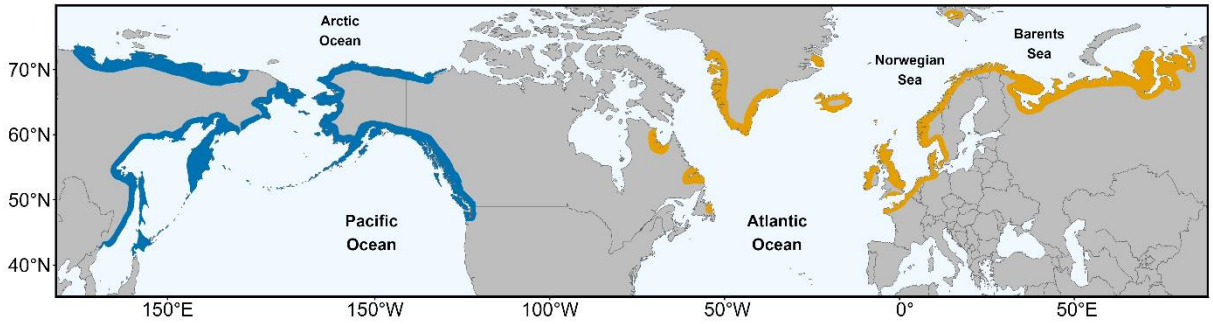

Sample collection

Otoliths were collected from 1116 Pink Salmon: 693 adults from the North Atlantic, 384 adults from the Pacific region (Alaska), and 39 juveniles from River Kongsfjord, northern Norway (Fig. 1; Table 1).

The samples from the North Atlantic were collected across a broad geographic range, including Norway, Greenland, Iceland, the Faroe Islands, Great Britain, and Ireland (hereafter termed "Atlantic region"). Since 1999 there has been no hatchery production of Pink Salmon in the Atlantic region, and all sampled fish were of wild origin. Fish were provided by recreational anglers or collected using traps in rivers. Of the 693 sampled adult Pink Salmon from the Atlantic region, both otoliths were available for mineral phase quantification from 610 fish, and one otolith available from a further 20 individuals. The remaining otoliths, that were broken but present, were classified as either aragonitic or vateritic but not included in the vaterite coverage analysis.

The samples from the Pacific region were provided by the Alaska Department of Fish and Game and were collected in 2021 using gillnets deployed in nearshore marine waters (Table 1). These fish represented a mixture of odd-year stocks returning to streams along the south-central Alaskan coast. Otoliths from 384 Pacific Pink Salmon were available (two otoliths from 326 individuals, and one from 58 individuals), of which 181 (47%) were identified as hatchery origin. At least one otolith from each pair was mounted on slides and polished to identify hatchery-origin individuals based on thermal marks. This process rendered the slide-mounted otoliths unusable for mineral phase quantification. As a result, 326 individuals (162 of wild origin and 164 of hatchery origin) had one intact otolith available for mineral phase quantification. Otoliths that were either mounted and polished or broken were classified as aragonitic or vateritic based on visual assessment.

Otolith mineral phase quantification

To classify and quantify calcium carbonate mineral phases, otoliths were imaged and processed for a pixel-based analysis. Each otolith was placed in a black microscopy bowl filled with ethanol (95 vol.%), positioned with the sulcus side up and the rostrum facing left. This orientation ensured that the dorsal side pointed upward for right otoliths, whereas the ventral side pointed upward for left otoliths (Fig. 2). Images were taken using a Leica MC170 HD camera attached to a Leica MZ 95 stereomicroscope and using Leica Application Suite X (LAS X) software (Leica Microsystems). Adult otoliths were imaged at 20–25× magnification and juvenile otoliths were imaged at 60× magnification. Both intact and broken otoliths were imaged, allowing visual classification of broken otoliths as either vateritic or aragonitic.

Images of intact otoliths were processed in Adobe Photoshop version 25.12.0 (Adobe Inc.), following the methodology described by Austad et al. (2021). Otolith outlines were selected using the quick select tool, with manual adjustments where necessary. The different mineral phases of calcium carbonate were manually classified by tracing the transitions between them, based on difference in texture and translucency, with vaterite appearing more transparent and cloudy, and aragonite exhibiting a more uniform, opaque structure. Different colors were assigned to aragonite and vaterite (Fig. 2), enabling a script to differentiate between them. After assigning the colors, the selected outlines were inverted, and the background was set to pure black to reduce pixel noise for the pixel-analysis. To quantify the coverage of each mineral phase, the "CountColor" package (Weller 2019) in R was used to count the pixels of each color while ignoring the background. These pixel counts were then used to estimate the proportion of the otolith surface composed of vaterite. For classification purposes, otoliths with any vaterite coverage (>0%) were classified as vateritic, whereas those without vaterite (0%) were classified as aragonitic. We also evaluated two alternative classifications, where otoliths with <10% and <33% vaterite were classified as aragonitic, with results provided in Table A1.

A version of each otolith image was also saved with the entire otolith structure filled in white (including both mineral phases) to facilitate subsequent shape and size analysis us-

Table 1. Number of examined individuals divided into regions, showing detailed counts for each sampling site, year of catch, and catch method.

Country—river	Sample size		Year of catch	Catch method	Collector*
Norway	**600**				
Børselv	21		2023	Trap	NINA
Børselv	116		2023	Bag net	NINA
Karpelva	5		2023	Trap	NINA
Komagelva	30		2023	Trap	NINA
Kongsfjord	87				
Juvenile		39	2022	Net	BJFF
Adult		48	2023	Trap	NINA
Kvalsund	15		2023	Trap	NINA
Lakselv	37		2023	Trap	NINA
Munkelv	26		2023	Trap	NINA
Repparfjord	30		2023	Trap	NINA
Skallelv	30		2023	Trap	NINA
Stabburselva	29		2023	Trap	NINA
Tana	14		2023	Trap	NINA
Vesterelva	32		2023	Trap	NINA
Vestre Jakobselv	29		2023	Trap	NINA
Namsen	4		2023	Trap	RA
Norwegian sea	85		2013–2023	Trawl	IMR
Stjørdalselva	2		2023	Trap	RA
Sylte-Moa	2		2023	Trap	RA
Numedalslågen	4		2021	Trap	RA
Sandvikselva	2		2021	Trap	RA
England	**15**				
NE England (costal)	11		2017, 2021	Nets	EA
R. Wear	3		2017	Rod	EA
R. Frome	1		2017	Rod	EA
Scotland	**19**				
R. Thurso	7		2021	Nets	FMS
R. Oykel	2		2019, 2021	Rod, Nets	FMS
R. Dee	10		2019, 2021	Spear gun, rod, found washed up	FMS
Ireland	**20**				
R. Moy	14		2021	Rod	IFI
R. Corrib	4		2021	Rod	IFI
R. Clare	1		2021	Rod	IFI
R. Erriff	1		2021	Trap	IFI
Faroe Islands	**10**				
Unknown	10		2021	Rod/Trawl	Firum/FAMRI
Iceland	**57**				
R. Bakká Bakkafirði	5		2021	Rod	MFRI
R. Berufjarðará	1		2017	Rod	MFRI
R. Botnsá	1		2021	Rod	MFRI
R. Brúará	3		2021	Rod	MFRI
R. Brunná	4		2021	Rod	MFRI
R. Fróðaá	1		2021	Rod	MFRI
R. Grímsá	1		2021	Rod	MFRI
R. Hamarsá	7		2017, 2023	Rod	MFRI

Table 1. (*concluded*).

Country—river	Sample size	Year of catch	Catch method	Collector*
R. Hrútafjarðará	1	2019	Rod	MFRI
R. Hvannadalsá	1	2021	Rod	MFRI
R. Krossá	1	2021	Rod	MFRI
R. Langa	1	2023	Rod	MFRI
R. Leirvogsá	1	2020	Rod	MFRI
R. Lýsuvötn	3	2021	Rod	MFRI
R. Miðfjarðará	1	2019	Rod	MFRI
R. Nordurá	4	2021	Rod	MFRI
R. Ólafsfjarðará	3	2021	Rod	MFRI
R. Rangá	1	2019	Rod	MFRI
R. Sléttuá	1	2021	Rod	MFRI
R. Sog	3	2021	Rod	MFRI
R. Stadará	4	2023	Rod	MFRI
R. Svarvaðardalsá	1	2019	Rod	MFRI
R. Vatnsdalsa	3	2023	Rod	MFRI
R. Ytri-Rangá	2	2020	Rod	MFRI
Unknown	3	2019–2023	Rod	MFRI
Greenland	**11**			
R. Kapisillit	4	2021	Spear gun	GINR
West Greenland	3	2017, 2021	Unknown	GINR
Napasoq	2	2021	Gill nets	GINR
Qorqut	1	2021	Rod	GINR
Tasiilaq	1	2017	Gill nets	GINR
Alaska, US	**384**			
Offshore	384	2021	Set gill nets	ADFG
Total	**1116**			

*NINA: Norwegian Institute for Nature Research, BJFF: Berlevåg Hunting and Fishing Association, RA: Recreational anglers, IMR: Norwegian Institute of Marine Research, EA: UK Environmental Agency, FMS: Fisheries Management Scotland, IFI: Inland Fisheries Ireland, FAMRI: Faroe Marine Research Institute, GINR: Greenland Institute of Natural Resources, MFRI: Icelandic Marine and Freshwater Research Institute, ADFG: Alaska Department of Fish and Game.

ing the ShapeR R-package (Libungan and Pálsson 2015). This was done to address the issue of poor contrast between the vateritic regions of the otolith and the background, which could otherwise hinder accurate shape extraction.

Validation of visual assessment using X-ray powder diffraction

To verify visual identification of calcium carbonate mineral phases in otoliths from adults, a subset of previously imaged otoliths ($n = 18$) was selected for XRD analysis. Otoliths were chosen to represent nearly the full range of vaterite coverage, spanning from 0% to 96% of total otolith area covered by vaterite, allowing for an evaluation of the method across the entire spectrum. Samples were carefully manually cleaned of organic material using fine forceps, rinsed with ethanol (95 vol.%), and air-dried.

Otoliths were crushed into a fine powder using a mortar and pestle and scanned for 90 min using a Bruker D8 A25 DaVinci X-ray Diffractometer with CuKα radiation (wavelength 1.54 Å). The LynxEye™ SuperSpeed Detector was configured with a scan range of 20°–80° 2θ and a step size of 0.013° 2θ (Table A2). A variable divergence slit was used to maintain a consistent illuminated width of 6 mm on the sample. Due to the limited amount of powder in each sample, an Si crystal cavity zero-diffraction plate sample holder with a 10 mm diameter and 0.2 mm deep cavity from MTI Corporation was used.

Raw diffraction patterns were analyzed using DIFFRAC.EVA software, version 6.0 (Bruker AXS, 2020) to identify the mineral phases of calcium carbonate present in every sample. The relative abundance of each mineral phase was then quantified using Rietveld refinement in DIFFRAC.TOPAS version 5.0 (Bruker AXS).

Otolith shape and morphological measurements

To investigate whether vaterite observed in adult Pink Salmon was initiated during the freshwater phase, the shape and size of otoliths from juvenile Pink Salmon collected in the River Kongsfjord prior to outmigration were analyzed.

Fig. 2. Pairs of otoliths from three individual Pink Salmon. Pair (*a*) shows two otoliths composed entirely of aragonitic. Pair (*b*) shows a difference in composition: the left otolith contains 83% vaterite, while the right otolith is fully aragonitic. Pair (*c*) shows similar composition in both otoliths, with vaterite dominating (98% in the left and 96% in the right). On the right side of the figure, the otolith pairs have been processed in Photoshop, with vaterite marked in blue and aragonite in orange for pixel-based quantification.

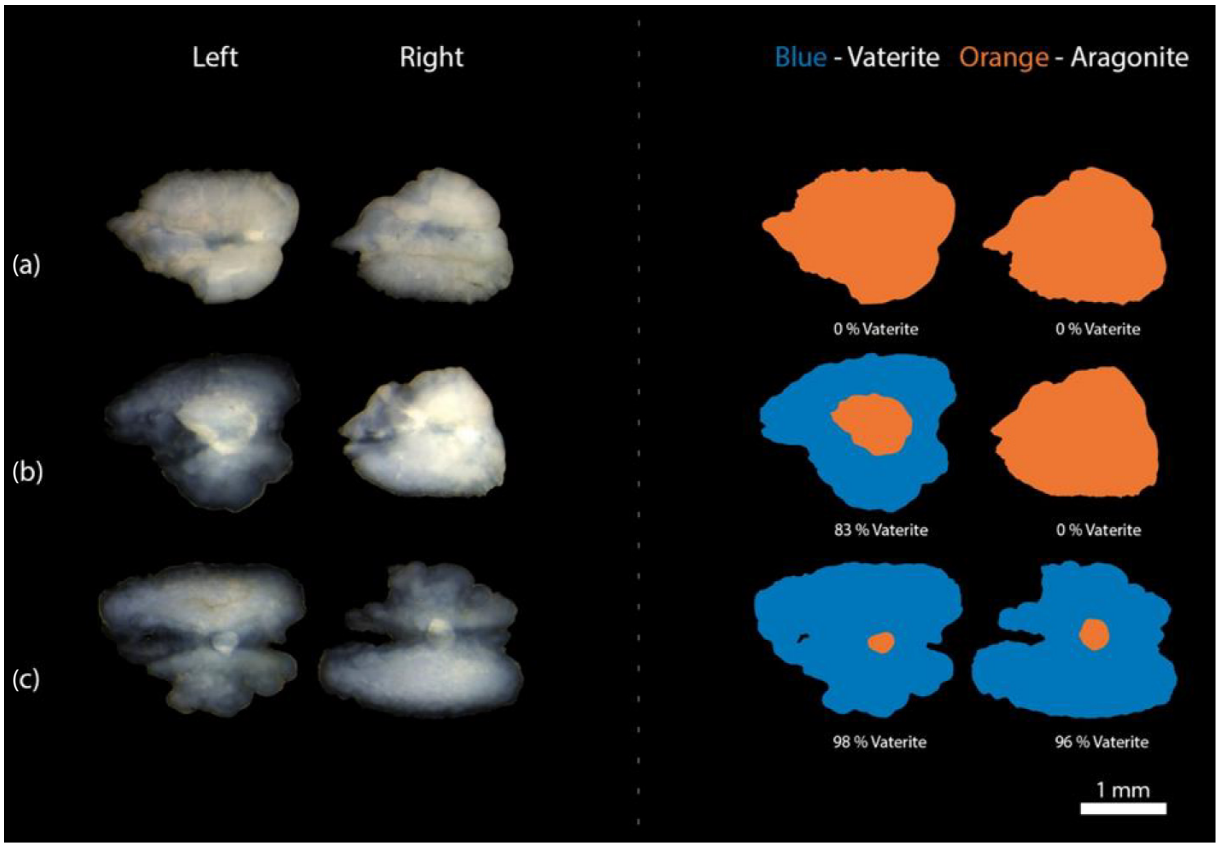

To ensure comparability between left and right juvenile otoliths, right otoliths were mirrored vertically prior to analysis. The ShapeR package in R (Libungan and Pálsson 2015) was used to retrieve the mean otolith shape from the high-contrast, black-and-white images. Mean otolith shape was reconstructed using Fourier descriptors, which standardize orientation and size by aligning otoliths along their longest axis and normalizing area.

Otolith length, width, area, and perimeter were quantified using the "getMeasurements" function. To characterize variability in juvenile otolith size, minimum, mean, and maximum values of otolith length and width were calculated (Table A3). These metrics were subsequently used to scale the mean juvenile otolith shape. Scaled juvenile otolith outlines, based on both mean and maximum juvenile dimensions, were used as a coarse estimate of the extent of freshwater growth prior to seawater entry. These outlines were overlaid onto adult otolith images to assess whether vaterite formation was present within regions corresponding to early growth (Fig. 3). This approach assumes that the outer boundary of juvenile otoliths approximates the position of the freshwater–seawater transition in adult otoliths. Minimum juvenile otolith dimensions were not used for scaling, as smaller individuals may not have reached the developmental stage associated with outmigration, and therefore could underestimate the extent of freshwater growth.

Juvenile otolith size varies among individuals and populations; thus, mean- and maximum-scaled outlines were used to provide a range of plausible transition positions rather than a precise estimate. The approach is qualitative and does not account for individual variability in migration timing.

Statistics

All data preparation and statistical analysis were performed using R, version 4.4.3 (R Core Team 2025) with graphical presentation generated using ggplot2 (Wickham 2009) and shapeR (Libungan and Pálsson 2015).

For the XRD method validation, a linear model was fitted with vaterite coverage estimated by visual assessment as the response variable, and vaterite coverage measured by XRD as the predictor variable. Model assumptions were evaluated by inspecting residual plots for homoscedasticity and normality (Fig. A1).

To assess whether the distribution of otolith pair types, AA (two aragonitic), VA (one aragonitic and one vateritic), and VV (two vateritic), differed among adult Pink Salmon from the

Fig. 3. (*a*) Juvenile Pink Salmon otolith mean shape reconstructed from Fourier coefficients. The reconstruction is grouped by left and right otoliths and plotted on top of each other. The plot shows negligible differences between left and right otolith. (*b*) Mean shape of juvenile otoliths scaled to mean and maximum length and width of juvenile otoliths from the present study overlaid on an adult otolith.

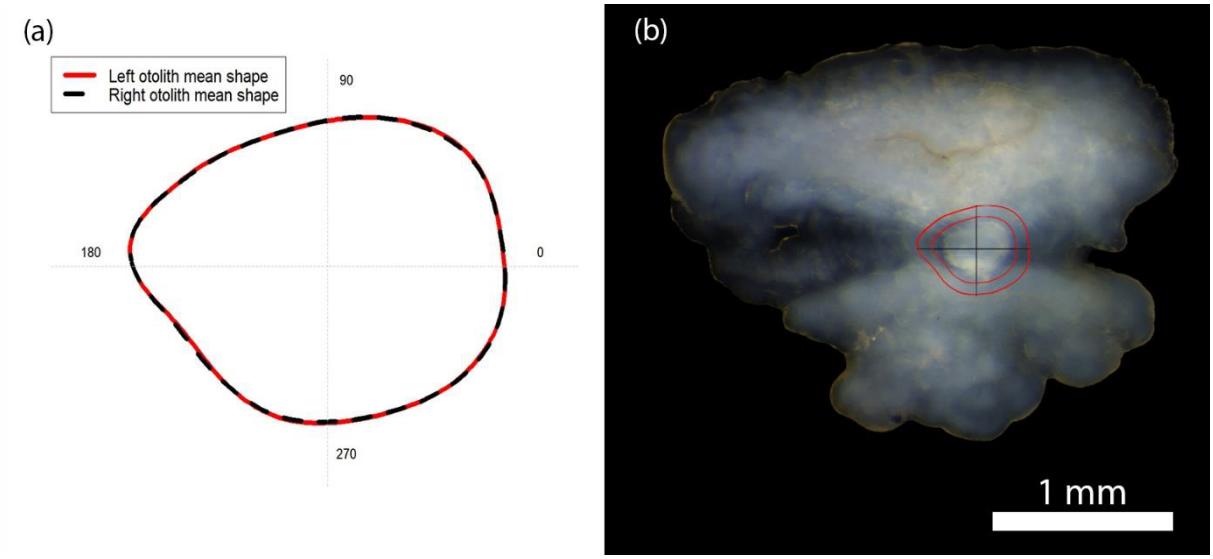

Atlantic region, Pacific region- wild group, and Pacific region-hatchery group, a Pearson's χ^2 test of independence was conducted using count data. A contingency table was constructed with the number of individuals assigned to each otolith type within each group. Standardized residuals were examined to identify which specific group–otolith type combinations contributed most to any significant differences observed.

To assess geographic differences in vaterite coverage between the Atlantic region group and the two Pacific region groups (hatchery and wild), we applied zero-inflated beta models using the glmmTMB package (Brooks et al. 2017). This approach was appropriate because vaterite coverage was measured as a proportion and included a substantial number of zeros (i.e., cases with no vaterite present). The modeling framework was selected for its ability to simultaneously account for two processes: (1) the presence or absence of vaterite, modeled using a zero-inflation component (logistic regression), and (2) the proportion of vaterite when present, modeled using beta regression (conditional component). For this analysis, vaterite coverage was quantified based on a single otolith per fish. For the Atlantic region fish, the right otolith was prioritized when available, while the left otolith was used if the right was missing. This approach was necessary because only the right otolith was available for mineral phase quantification in the Pacific region samples. Four versions of the zero-inflated beta model were fitted, each differing in the inclusion of group effects (Atlantic, Pacific wild, Pacific hatchery) in the conditional and/or zero-inflation components. Model selection was performed using the "mod.sel" function from the MuMIn package (Barton 2024), based on Akaike's information criterion. The inverse logit function was used to interpret the model estimates, and the reference level for the group variable was adjusted to obtain accurate confidence intervals for each group. Model assumptions were evaluated through visual inspection of plots from the DHARMa package (Hartig 2024), focusing on dispersion, uniform distribution of the residuals, outliers, and group-level variability (Fig. A2).

Results

Validation of visual assessment using X-ray powder diffraction

The XRD data showed characteristic peaks corresponding to vaterite (PDF 00-069-0001) and aragonite (PDF 04-006-5441), with least-square values for Rietveld refinement, expressed as the weighted profile R-factor, ranging from 6.68 to 12.61. The linear model revealed a highly significant relationship between vaterite coverage based on visual assessment and XRD-derived vaterite coverage (Table A4), with a regression slope of 0.96 (Fig. 4). The mean absolute deviation between the two methods was 2.88% (SD $\pm$ 2.28%), with a maximum deviation of 6.89%. These findings suggest that visual assessment aligns closely with XRD measurements.

To evaluate the repeatability of the visual assessment, 40 randomly selected otolith images were reprocessed in Photoshop and compared with the initial visual assessment, yielding highly consistent results ($R^2 = 0.99$, $p < 0.001$). Both the repeatability and XRD analyses confirm that visual assessment provides an accurate and reproducible method for estimating vaterite in Pink Salmon otoliths, with minimal deviation from XRD validation.

Prevalence of vaterite in Pink Salmon otoliths

A high prevalence of vaterite was observed in both regions, with vaterite present in one or both otoliths in 97% of the 610

Fig. 4. Scatter plot with a 1:1 line (dashed line) and fitted line (solid line) illustrating the linear relationship between visually assessed vaterite coverage and X-ray diffraction (XRD)-derived vaterite coverage ($n = 18$). $y = 0.959x + 0.026$, $R^2 = 0.987$, $p < 0.001$. The shaded area represents the 95% confidence interval (slope CI = 0.91–1.01).

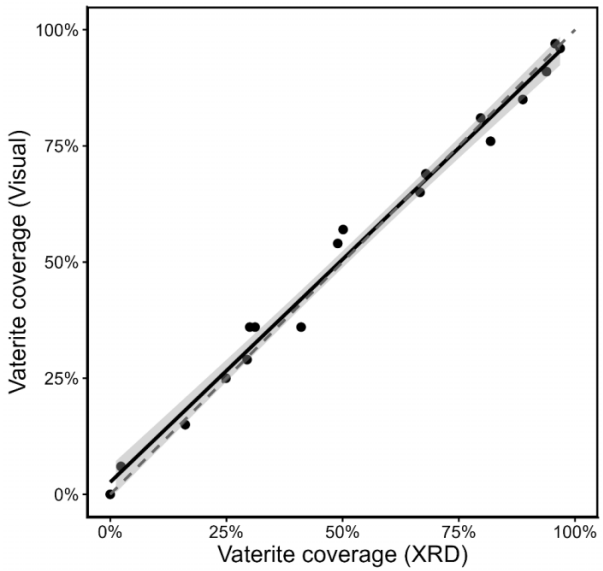

Atlantic Pink Salmon and 95% of the 276 Pacific Pink Salmon examined.

Juveniles

It was challenging to visually assess whether juvenile otoliths had initiated the formation of vaterite due to their small size. Among the examined otoliths ($n = 51$), at least two showed signs of vaterite development (Fig. A3). The core area of all juvenile otoliths was composed of the aragonite mineral phase. However, the juvenile otoliths were too small to be analyzed with XRD, as they did not yield sufficient powder per sample to meet the analytical requirements.

Adults

Atlantic region

Among the adult Pink Salmon sampled from the Atlantic region, only 3% of the fish had two otoliths without any vaterite, 84% had vaterite present in both otoliths, while 13% had vaterite present in only one otolith. Vateritic otoliths were observed in samples from all the Atlantic countries (Table 2).

Pacific region—hatchery origin

Among the hatchery origin Pink Salmon from the Pacific region, only 6% of the fish had two otoliths without any vaterite, 69% had vaterite present in both otoliths, while 25% had vaterite present in only one otolith (Table 2).

Pacific region—wild origin

Among the wild origin Pink Salmon from the Pacific region, only 4% of the fish had two otoliths without any vaterite, 76% had vaterite present in both otoliths, while 20% had vaterite present in only one otolith (Table 2).

Comparing groups

The distribution of otolith types differed among the three groups (chi-squared test, $\chi^2 = 22.36$, df = 4, $p < 0.001$). Standardized residuals indicated that the Pacific hatchery group had significantly more fish with one vateritic otolith and one aragonitic otolith than expected (standardized residual = 3.49), and significantly fewer fish where both otoliths were vateritic (−4.03). In contrast, the Atlantic group had significantly fewer fish with one vateritic otolith than expected (−3.99), and significantly more with two vateritic otoliths (4.34). No other group–otolith combinations exceeded the threshold for statistical significance ($z > \pm 1.96$).

Vaterite coverage in adult Pink Salmon otoliths

Across all groups (Atlantic region, Pacific hatchery, Pacific wild), vaterite coverage ranged from 0% to 99%. There were peaks in the distribution at 0% and ~80% (Fig. 5). Coverage was quantified from a single otolith per fish (Atlantic $n = 630$; Pacific $n = 326$). In adult fish with two intact otoliths, there was no systematic difference in vaterite coverage between left and right otoliths (paired t test, $t = 0.53$, df = 425, $p = 0.60$: Fig. A4).

There was some variation in mean vaterite coverage between countries in the Atlantic region; Iceland 46% (range: 0%–92%), England 44% (range: 6%–87%), Faroe Islands 45% (range: 8%–92%), Greenland 51% (range: 1%–93%), Ireland 48% (range: 0%–94%), Scotland 59% (range: 7%–89%), and Norway 49% (range: 0%–99%). Due to the small country-level sample size, no statistical comparisons were made within the Atlantic group. Both Pacific hatchery and wild-origin fish exhibited similar distributions of vaterite coverage, similar to the pattern observed in the Atlantic region; however, wild fish had an additional peak at ~30% vaterite coverage (Fig. 5).

Differences between Atlantic and Pacific populations

Model selection supported the inclusion of group effects in the zero-inflation component of the model, whereas evidence for a group effect in the conditional component was weaker (Table 3). The two top-ranked models included group as a predictor in the zero-inflation component, with the best model (gv_2) also including group as a predictor in the conditional component. However, the difference in AICc between gv_2 and the simpler model gv_3 was small (ΔAICc = 0.72), suggesting limited additional explanatory power from including group as a predictor in the conditional component.

Examination of model estimates confirmed differences between groups in the zero-inflation component, with a large effect size, supporting the inclusion of a group effect in the zero-inflated component. In contrast, although the conditional component showed a group effect, the effect size

Table 2. Numbers of Pink Salmon with two aragonitic (AA), one aragonitic and one vateritic (VA), and two vateritic (VV) otoliths in sampled Pink Salmon from the Atlantic region and Pacific region.

Location	AA	VA	VV	Total
Norway	19 (4)	67 (13)	431 (83)	517
Great Britain and Ireland	0	2 (5)	36 (95)	38
Faroe Islands	0	0	10 (100)	10
Iceland	1 (3)	7 (19)	28 (78)	36
Greenland	0	0	9 (100)	9
Total Atlantic region	**20 (3)**	**76 (13)**	**514 (84)**	**610**
Pacific hatchery	11 (6)	44 (25)	122 (69)	177
Pacific wild	8 (4)	39 (20)	152 (76)	199
Total Pacific region	**19 (5)**	**83 (22)**	**274 (73)**	**376**

Note: Numbers in parentheses represent percentage of total count.

Fig. 5. Distribution of vaterite coverage (% vaterite in individual otoliths) divided into three groups of Pink Salmon: Atlantic region, Pacific region—wild origin, and Pacific region—hatchery origin. The far-left bar illustrates the otoliths without vaterite. Red dashed lines represent the estimated mean from model gv_2.

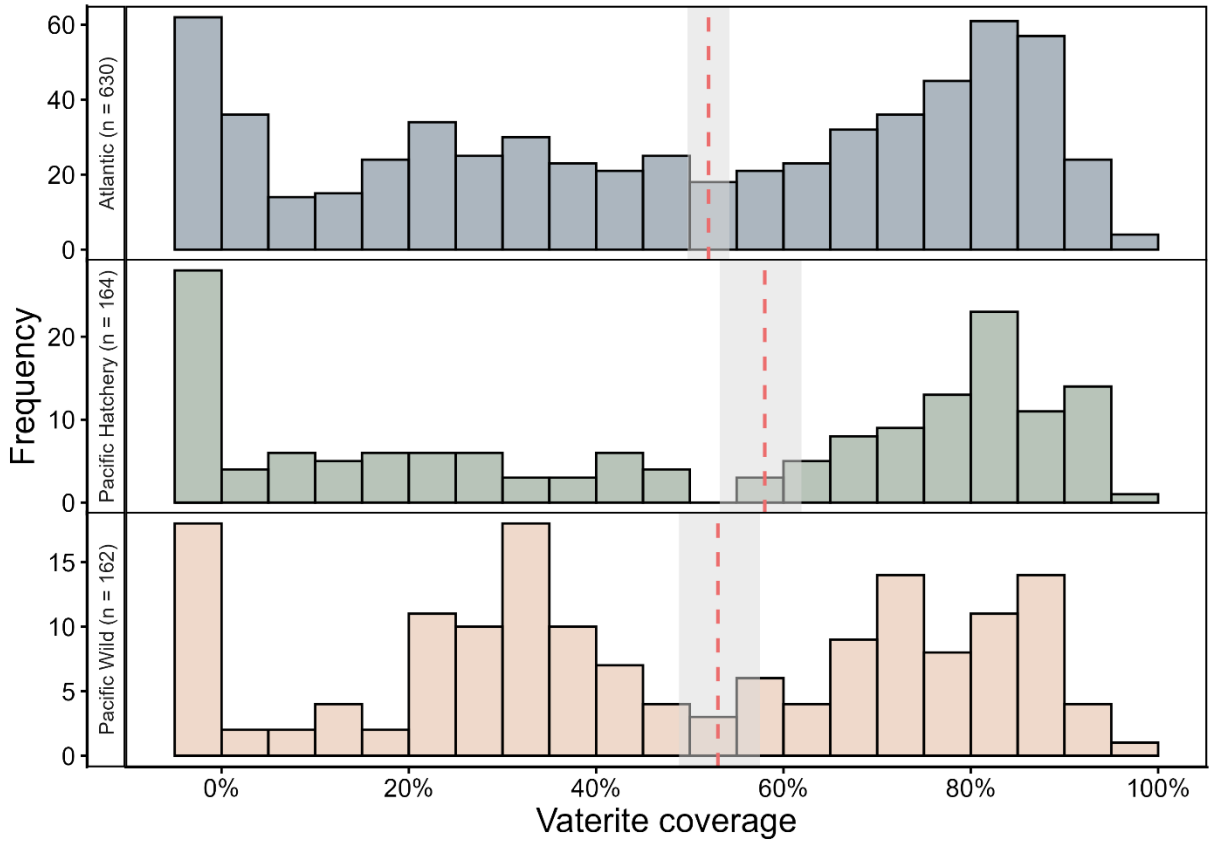

was small, suggesting that the proportion of vaterite (when present) did not vary substantially between groups (Table 4).

The zero-inflated component showed that the Pacific hatchery group had a higher proportion of zeros compared with the two wild groups ($p = 0.01$), with 17.1% (95% CI: [12%–24%]) zeros compared with 9.8% (95% CI: [8%–12%]) and 11.1% (95% CI: [7%–17%]) in the Atlantic and Pacific wild, respectively. For the conditional component, two models were within a ΔAICc of 0.72. For the model including group as a predictor in the conditional component (gv_2), the Pacific hatchery group had the highest mean vaterite coverage at 58% (95% CI: [53%–62%]), significantly different from the Atlantic group at 52% (95% CI: [50%–54%]), and the pacific wild group at 53% (95% CI: [49%–57%]). In the model where we did not include group as a predictor in the conditional component (gv_3), the model estimated that the mean percentage coverage of all the included Pink Salmon was 53% (95% CI: [51%–55%]).

Table 3. Model comparison of four zero-inflated beta models investigating geographical differences (gv) in vaterite coverage (prop_vat) of Pink Salmon.

Model	Conditional component	Zero-inflated component	df	AICc	ΔAICc
gv_2	prop_vat ~ pop	~pop	7	657.7	0.00
gv_3	prop_vat ~ 1	~pop	5	658.4	0.72
gv_1	prop_vat ~ pop	~1	5	659.8	2.15
gv_4	prop_vat ~ 1	~1	3	660.6	2.89

Note: pop: grouping variable (Atlantic, Pacific wild, and Pacific hatchery).

Table 4. The top two models testing whether the prevalence of vaterite and mean vaterite coverage differ between groups of Pink Salmon.

Model	Variable	Estimate	SE	*z*-value	*p*-value
gv_2	**Conditional component**				
	(Intercept)	0.08589	0.04457	1.927	0.0540
	Pacific hatchery	0.22159	0.10152	2.183	0.0291
	Pacific wild	0.04168	0.09906	0.421	0.6739
	Zero-inflated component				
	(Intercept)	−2.2150	0.1338	−16.560	<0.001
	Pacific hatchery	0.6345	0.2469	2.570	0.0102
	Pacific wild	0.1355	0.2835	0.478	0.6326
gv_3	**Conditional component**				
	(Intercept)	0.12844	0.03659	3.510	<0.001
	Zero-inflated component				
	(Intercept)	−2.2150	0.1338	−16.560	<0.001
	Pacific hatchery	0.6345	0.2469	2.570	0.0102
	Pacific wild	0.1355	0.2835	0.478	0.6326

Note: All parameter estimates are reported on the logit scale.

Onset of vaterite formation in Pink Salmon otoliths

Signs of vaterite within the putative freshwater growth region were assessed by comparing scaled juvenile otolith outlines (based on mean and maximum juvenile dimensions; Table A3) with adult otolith images (Fig. 3). Among 111 Atlantic-region otoliths with ≥80% vaterite coverage, 25 individuals showed vaterite within the area defined by the maximum scaled juvenile outline, while 6 showed vaterite within the area defined by the mean scaled outline. Vaterite coverage in individuals identified using the maximum scaled outline ranged from 90% to 99%, with most ($n = 19$) exhibiting ≥95% coverage, whereas all individuals identified using the mean scaled outline had vaterite coverage of ≥96%.

To complement the overlay analysis, a qualitative comparison was conducted using a subset of mounted and polished adult otoliths ($n = 10$), all from River Kongsfjord. Scaled juvenile outlines showed general visual correspondence with the darker central region of the otoliths (Fig. 6). In 7 of the 10 samples, alignment was closest to the maximum-scaled outline, while 2 aligned more closely with the mean-scaled outline and 1 fell between the two. When applying both mean- and maximum-scaled outlines, variation among individuals became evident, suggesting that the timing of sea entry differs between individuals and highlighting the sensitivity of the method to assumptions about juvenile size. Consequently, the presence of vaterite within this region should be interpreted cautiously, as the timing of seawater entry cannot be determined with precision using this approach alone.

Fig. 6. (*a*) Mounted and polished adult otolith showing the putative freshwater growth region at the center. (*b*) Mean juvenile otolith shape overlaid and scaled to the maximum (outer ring), mean (middle ring), and minimum (inner ring) otolith measurements of juveniles from the present study.

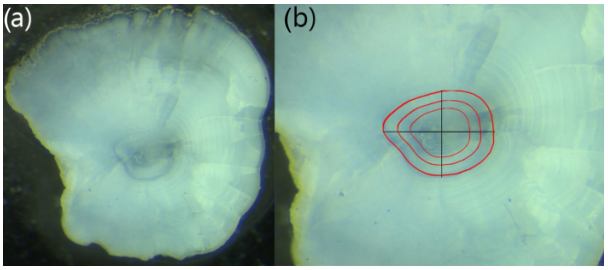

Discussion

This study provides novel insights into the prevalence of vateritic otoliths in Pink Salmon, addressing knowledge gaps in both native and invasive populations. The results indicate that nearly all Pink Salmon surviving a year at sea return

to the coast and rivers with some degree of vaterite in at least one otolith. In addition, vaterite formation appears to occur across multiple life–history stages, beginning as early as the freshwater juvenile phase and continuing into the marine phase. Visual assessment of otolith mineralogy was also shown to be a precise and time-efficient method for classifying mineral phases, offering a valuable screening tool for future research.

Prevalence of vaterite in Pink Salmon otoliths

The occurrence of vaterite in salmonids has gained increasing attention in recent years, primarily due to its detrimental effects on otolith functionality and potential implications for fish welfare, particularly in hatchery and aquaculture settings (Reimer et al. 2016, 2017; Austad et al. 2021; Gaffney et al. 2025). Numerous studies have associated hatchery conditions with increased prevalence of vaterite (Reimer et al. 2016; Gaffney et al. 2025), raising concerns about the performance and survival of hatchery-reared fish upon release into the wild. Despite this growing body of literature, Pink Salmon remain understudied in this context, resulting in a notable knowledge gap considering the baseline prevalence of vaterite in wild populations.

In the present study, the prevalence of vaterite was consistently high across Atlantic and Pacific groups, regardless of wild or hatchery origin. Specifically, 97% of Atlantic region fish and 95% of Pacific region fish exhibited some level of vaterite, a difference between the two groups likely to be within the margin of error given the methodology. Pacific region hatchery fish were roughly 1.5–1.7 times more likely to have at least one aragonitic otolith than fish from the two wild groups. This finding is somewhat unexpected, because hatchery fish are generally considered more prone to developing vateritic otoliths (Reimer et al. 2016; Gaffney et al. 2025). The shorter hatchery-rearing period of Pink Salmon than other salmonid species may be one factor contributing to the different relationship between wild and hatchery origin fish observed in this species. Explaining the difference between the wild and hatchery origin Pink Salmon is challenging without further investigation into how their life histories differ. One possibility is that hatchery fish in this region experience lower stress levels than their wild counterparts, potentially reducing vaterite formation. Given that vaterite prevalence can vary substantially among hatcheries (Gaffney et al. 2025), firm conclusions are difficult without detailed information on hatchery practices associated with these fish.

A key concern associated with vaterite formation is its potential impact on auditory function. Oxman et al. (2007) reported reduced hearing sensitivity in fish with one or two vateritic otoliths, but classified otoliths with <33% vaterite as functionally aragonitic. This interpretation has been reconsidered by later work suggesting that the effects of vaterite coverage may be progressive rather than threshold-based. For instance, Reimer et al. (2016) showed that increasing vaterite coverage was associated with reduced otolith oscillation amplitude, indicating the potential for gradual effects on hearing function.

Given the absence of a clearly defined biological threshold, we explored the sensitivity of our results to alternative classification criteria (0%, 10%, and 33% vaterite coverage). Increasing the threshold led to changes in absolute parameter estimates (Table A1), particularly in the zero-inflated component, as expected. However, the relative differences among groups were broadly similar across thresholds, and the overall patterns in the conditional component were retained. Applying a 33% threshold, consistent with Oxman et al. (2007), did not lead to substantive changes in the interpretation of group-level differences.

Although some differences were observed in the statistical components, their biological significance is uncertain. Together, these results suggest that the main findings are relatively insensitive to the choice of classification threshold. Therefore, we retained the presence/absence definition in the main analyses to facilitate comparison with previous studies, while acknowledging that the absence of a biologically defined cutoff remains a limitation. Hearing impairment could theoretically impact key behaviors such as navigation, predator avoidance, and foraging. Although Pink Salmon generally return to natal rivers to spawn, their homing precision may be lower than that of other salmonids (Quinn 1993, 2018). Most studies report straying rates below 5%–10%, with many individuals homing back to remarkably fine-scale locations within their natal river, though rates as high as 50% have been observed (Sharp et al. 1994; Thedinga et al. 2000; Mortensen et al. 2002; May et al. 2023). The fact that most returning spawners in our study exhibited extensive vaterite coverage indicates that Pink Salmon are still able to complete their spawning migrations despite altered otolith structure. This suggests that vateritic otoliths are unlikely to play a major role in determining broad-scale homing ability, which may not be surprising given that other cues, such as geomagnetic navigation, are thought to be the primary drivers for homing (Putman et al. 2014). In broader terms, Pink Salmon are schooling fish and may benefit from the group for predator avoidance, food finding, and possibly homing. So those with compromised sensory faculties could possibly benefit from this group dynamic.

When compared with other salmonids, the Pink Salmon exhibits an exceptionally high prevalence of vaterite (Fig. 7). The closest comparison is farmed Atlantic salmon (*Salmo salar*, Linnaeus, 1758) at harvest size, where Reimer et al. (2017) observed vaterite in 100% of individuals from one population. Nonetheless, wild Pink Salmon exceeds most other species, including hatchery-origin fish, in the prevalence of vaterite. In contrast to findings in other salmonids, no clear distinction was observed between hatchery- and wild-origin Pink Salmon.

Several studies suggest that rapid growth promotes vaterite development in salmonids. For example, Reimer et al. (2017) experimentally induced vaterite in 90% of otoliths in Atlantic salmon by manipulating water temperature and light conditions to accelerate growth, with temperature having the strongest effect. The link between rapid growth and increased vaterite prevalence is supported by consistently higher vaterite levels in hatchery-reared fish compared with wild counterparts across multiple salmonid species (Fig. 7).

Fig. 7. Comparison of vaterite prevalence across salmonids. Each colored point (open = juvenile, filled = adult) represents a studied population, categorized as wild, hatchery, or farmed origin. Farmed fish are defined as individuals reared in captivity for their entire life, whereas hatchery fish are released into the wild at the juvenile stage. Black points represent group means, and error bars indicate standard deviation within each group.

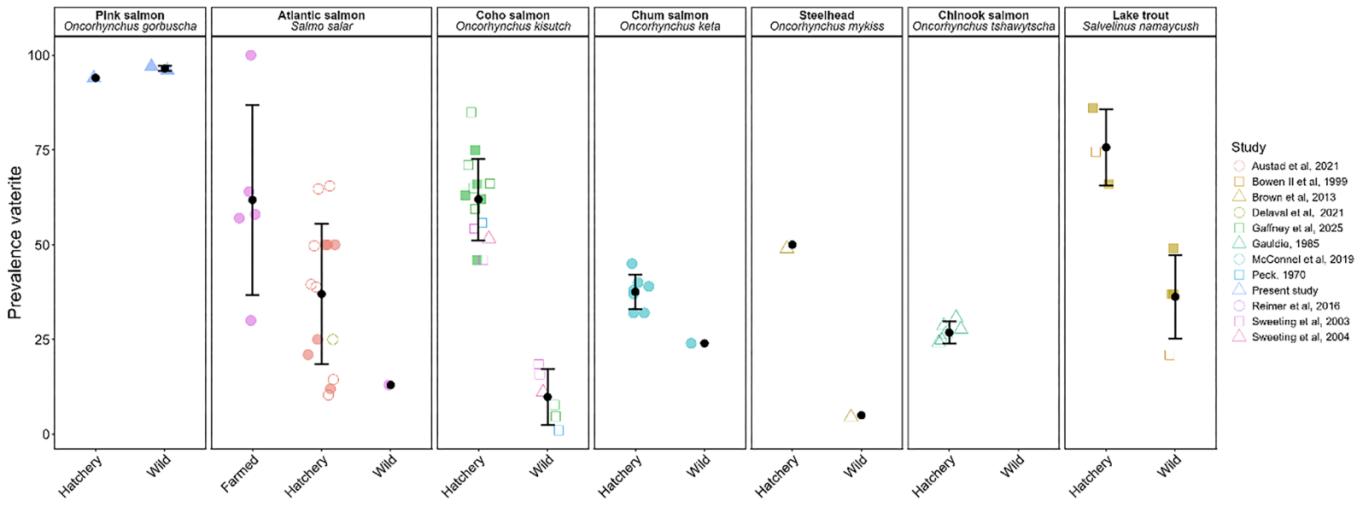

Notably, farmed Atlantic salmon, which are known for their fast growth, exhibit the second highest prevalence of vaterite, surpassed only by Pink Salmon, which grow even more rapidly. They grow from fry measuring just 3–5 cm in length, typically <1 g (Erkinaro et al. 2023) to adults weighing 0.5–4.0 kg within just 14–15 months at sea. Comparative studies under Norwegian aquaculture conditions (Gjedrem and Gunnes 1978) have also shown that Pink Salmon outgrow other salmonids, including Atlantic salmon, Arctic charr (*Salvelinus alpinus*, Linnaeus, 1758), and sea trout (*Salmo trutta*, Linnaeus, 1758). Such growth rates may therefore be a key factor contributing to the high prevalence of vaterite observed in Pink Salmon. However, not all studies have found a direct relationship between growth and vaterite formation. While Delaval et al. (2021) and Reimer et al. (2017) linked high growth rate to increased vaterite occurrence, Austad et al. (2021) found no such relationship and, instead, pointed to stress and crowding as important drivers. These contrasting findings indicate that vaterite formation likely reflects a complex interplay of biological and environmental factors, including life–history characteristics such as early sea migration in Pink Salmon, which may potentially contribute to vaterite development. Nevertheless, the consistently high prevalence of vaterite in Pink Salmon across different origins observed in the present study suggests that species-specific physiological and life–history traits, such as their unique growth rate and rapid out-migration, may be a key driver of vaterite formation.

Vaterite coverage and onset of vaterite formation

When vaterite was present, the average otolith area covered by vaterite differed significantly between the Atlantic and Pacific populations. However, the small effect size suggests limited biological relevance. The distribution of vaterite coverage was characterized by several distinct peaks at approximately 80%, 30%, and 0% coverage, indicating that mean values may not adequately capture the underlying variation. These peaks likely correspond to specific events or life stages during/after which vaterite formation becomes more pronounced and, therefore, may provide more informative insights than average values alone. Given that vaterite formation is believed to be irreversible, the histogram of vaterite coverage (Fig. 5) could be interpreted as a timeline of otolith development, where 100% coverage represents vaterite from early in life. Previous studies support the idea that vaterite formation is often triggered relatively early in life. For example, Bowen et al. (1999) observed a distinct peak in vaterite coverage around 80% in hatchery-reared lake trout (*Salvelinus namaycush* (Walbaum, 1792)) and attributed this to early onset, likely during critical developmental periods when the otolith is particularly sensitive to stress.

Further evidence for early vaterite formation comes from 25 otoliths showing vaterite within the juvenile overlay region, suggesting it may begin during the freshwater stage. Similarly, Delaval et al. (2021) reported that some Atlantic salmon began forming vaterite within 6 weeks of first feeding under hatchery conditions. In addition to freshwater onset, the early marine period may represent another critical window for vaterite formation. Offshore samples collected in December (6–8 months at sea) provide valuable clues. In the December samples, vaterite covered an average of 37% of the otolith surface, with individual values ranging from 0% to 75%, suggesting that vaterite formation had already been underway in many fish for some time. Given that juvenile Pink Salmon typically remain in nearshore habitats for several weeks to months before migrating offshore, the December otoliths support the interpretation that vaterite onset in a substantial proportion of the population occurs during the early marine phase. The shift in environment, which includes exposure to new threats and changes in osmoregulation, tem-

perature and growth rate, may act as stressors responsible for triggering this mineralogical shift.

The abundance of fish with approximately 30% vaterite coverage is difficult to interpret without knowing the specific timing and conditions during this life stage. One possibility is that it reflects a second period of elevated stress or rapid growth. Scale-based studies of Pink Salmon suggest several periods of rapid growth separated by slower growth during the marine phase, particularly one period with slow growth in the late summer/early autumn, and one period during the winter (Paulsen et al. 2022; Kaev et al. 2023; Simmons et al. 2026). It is possible that this pattern corresponds with the two peaks in vaterite coverage seen in the present study, with the 30% vaterite peak associated with the rapid growth phase after the first period of slow growth. If true, this would support the idea that growth rate may influence the likelihood of vaterite formation, as suggested by Delaval et al. (2021) and Reimer et al. (2017). However, further work is required to establish any correlation between growth rate and vaterite coverage.

Validation of visual assessments using X-ray powder diffraction

A strong positive linear relationship was observed between visually assessed and XRD-derived vaterite coverage, demonstrating that visual quantification provides a highly accurate estimate of bulk otolith mineralogy in Pink Salmon. The regression slope did not differ significantly from unity, indicating an absence of systematic bias in visual assessments. Visual estimates explained 99% of the variation in vaterite proportion measured by XRD, showing that two-dimensional image-based assessments reliably reflect bulk mineral composition in this species.

This result is particularly significant because XRD is a destructive, time–consuming, and relatively costly analytical technique, whereas visual assessment is rapid, inexpensive, and non–destructive. Our findings demonstrate that visual screening provides a reliable alternative for quantifying otolith vaterite content, particularly when large sample sizes are required. This has clear practical relevance for fisheries science, where the ability to efficiently process large numbers of otoliths is often a limiting factor. Moreover, the presence of vaterite can severely compromise the readability of otoliths, as both thermal mark identification and daily increment analysis are often difficult or not possible in vateritic otoliths.

Few studies have directly validated visual assessments of otolith mineralogy against XRD, and to our knowledge this is the first study to apply and compare both methods in Pink Salmon. One of the few comparable studies is that of Lewis et al. (2022), who validated visual assessments against XRD in delta smelt (*Hypomesus transpacificus,* McAllister, 1963) and likewise reported strong agreement between methods ($R^2 = 0.84$). Together, these findings suggest that image–based visual assessment can provide a precise estimate of otolith mineral composition across species. Additionally, several studies have successfully applied visual, image–based approaches to characterize otolith mineralogy (e.g., Austad et al. 2021; Gaffney et al. 2025), supporting the broader applicability of this method. We propose that visual assessment may be broadly reliable in species with comparable otolith morphology, as the principal calcium carbonate polymorphs exhibit distinct and consistent visual characteristics.

Overall, this validation highlights the utility of visual assessment as an effective screening tool for otolith mineralogy and supports its wider application in studies of vaterite occurrence, hatchery impacts, and daily increment analysis.

Conclusions

This study provides new insights into the occurrence and development of vaterite in Pink Salmon. A key finding is that Pink Salmon has a remarkably high prevalence of vaterite compared with other salmon species, even surpassing the prevalence in hatchery reared populations. No differences were found between native and invasive populations of Pink Salmon regarding otolith minerology; however, patterns indicate a higher frequency of asymmetrical otolith pairs among hatchery-origin Pink Salmon, which requires closer examination. Results indicate that vaterite formation can begin as early as the freshwater stage in juvenile Pink Salmon, with patterns suggesting distinct periods in the life cycle when the transition from aragonite to vaterite becomes more pronounced, possibly linked to growth rate. Future studies could investigate relationships between vaterite formation and growth rate, both within Pink Salmon and across species, to clarify how growth dynamics influence otolith mineralogy. Additionally, exploring potential links between vaterite and homing behavior or dispersal, through the integration of genetic and geochemical approaches, could offer deeper insights into the ecological and physiological significance of vaterite in Pink Salmon. Overall, the findings support the hypothesis that the exceptionally high prevalence of vaterite in Pink Salmon may be a consequence of their life history strategy characterized by rapid growth over a two-year cycle. While no direct relationship between vaterite and size was detected in the present dataset, this may reflect a lack of variation in growth rates, rather than the absence of an underlying biological mechanism. If rapid growth indeed increases the likelihood of vaterite formation, it may come at a physiological cost, potentially including hearing impairment, raising important questions about trade-offs in the evolution of growth strategies among salmonids.

Acknowledgements

We are grateful to Elvia Anabela Chavez Panduro for her training and guidance during the X-ray diffraction analysis. We would like to thank the Berlevåg Jeger-og Fiskerforening for giving us access to the Pink Salmon trap in the River Kongsfjord and their assistance in the field for collecting juvenile otoliths. We thank Eydna í Homrum and the Faroe Marine Research Institute, Alan Youngson at the University of the Highlands and Islands, and Paul Hopper at the Outer Hebrides Fisheries Trust for contributing samples. Furthermore, we thank Randi J. Saksgård for extracting juvenile otoliths. We are deeply appreciative of all individuals who volunteered

their time for field collection of Pink Salmon in the different areas. Finally, we would like to thank the Associate Editor, Micah Quindazzi and an anonymous reviewer for their constructive comments that helped improve the manuscript.

Article information

History dates

Received: 6 March 2026
Accepted: 7 July 2026
Accepted manuscript online: 10 August 2026

Copyright

© 2026 The Authors. This work is licensed under a Creative Commons Attribution 4.0 International License (CC BY 4.0), which permits unrestricted use, distribution, and reproduction in any medium, provided the original author(s) and source are credited.

Data availability

The data and R scripts used to reproduce the analyses and figures presented in this article have been deposited in Zenodo and are available at https://doi.org/10.5281/zenodo.21413797.

Author information

Author ORCIDs

Frode Pedersen https://orcid.org/0009-0005-7262-9611
Henrik H. Berntsen https://orcid.org/0000-0002-4074-3525
Eva B. Thorstad https://orcid.org/0000-0002-7373-6380
Michał E. Skóra https://orcid.org/0000-0002-9121-1318
J. Iwan Jones https://orcid.org/0000-0002-7238-2509
Sigurd Einum https://orcid.org/0000-0002-3788-7800
Kirstin Eliasen https://orcid.org/0009-0009-4592-4227
Michael Millane https://orcid.org/0000-0003-2839-7671
Kjell R. Utne https://orcid.org/0000-0002-6428-3690
Malte Willmes https://orcid.org/0000-0001-8734-5324

Author contributions

Conceptualization: FP, HHB, EBT, SE, MW
Data curation: FP, HHB, EBT, SE, MW
Formal analysis: FP, HHB, EBT, SE, MW
Funding acquisition: HHB, EBT, MES, JIJ, SE, MW
Investigation: FP, HHB, EBT, SE, MW
Methodology: FP, HHB, EBT, SE, MW
Project administration: FP, HHB, EBT, SE, MW
Resources: HHB, EBT, MES, JIJ, GDD, SE, KE, GG, NSJ, MM, JN, EOO, DSO, SR, JU, KRU, MW
Supervision: HHB, EBT, SE, MW
Validation: FP, HHB, EBT, MES, JIJ, SE, EOO, DSO, MW
Visualization: FP, HHB, EBT, SE, MW
Writing – original draft: FP, HHB, EBT, SE, MW
Writing – review & editing: FP, HHB, EBT, MES, JIJ, GDD, SE, KE, GG, NSJ, MM, JN, EOO, DSO, SR, JU, KRU, MW

Competing interests

The authors declare no conflicts of interest.

Funding information

Funding to prepare this article was provided by the Norwegian Institute for Nature Research and Eva B. Thorstad, Henrik H. Berntsen, Narve Stubbraaten Johansen, and Malte Willmes also received funding from the Research Council of Norway, project No. 160022/F40. Michał E. Skóra's work was funded by the European Union's Horizon 2020 Research and Innovation Programme under the Marie Skłodowska-Curie grant agreement No. 101026030. J. Iwan Jones' work was funded by the Natural Environment Research Council Arctic Office. Project: Establishing the origin of the invasive Pink Salmon, *Oncorhynchus gorbuscha*, spawning in Icelandic rivers.

References

Augerot, X. 2005. Atlas of Pacific salmon: the first map-based status assessment of salmon in the North Pacific. University of California Press.

Austad, B., Vøllestad, L.A., and Foldvik, A. 2021. Frequency of vateritic otoliths and potential consequences for marine survival in hatchery-reared Atlantic salmon. J. Fish Biol. **98**(5): 1401–1409. doi:10.1111/jfb.14683.

Barton, K. 2024. MuMIn: multi-model inference (Version 1.48.4) [R package]. Available from https://CRAN.R-project.org/package=MuMIn.

Bowen, C.A., Bronte, C.R., Argyle, R.L., Adams, J.V., and Johnson, J.E. 1999. Vateritic Sagitta in wild and stocked lake trout: applicability to stock origin. Trans. Am. Fish. Soc. **128**(5): 929–938. doi:10.1577/1548-8659(1999)128≤0929:VSIWAS≥2.0.CO;2.

Brandt, J.E., Wesner, J.S., Ruggerone, G.T., Jardine, T.A., Eagles-Smith, C.A., Ruso, G.E., et al. 2024 Continental-scale nutrient and contaminant delivery by Pacific salmon. Nature, **634**: 875–882. doi:10.1038/s41586-024-07980-2.

Brooks, M.E., Kristensen, K., van Benthem, K.J., Magnusson, A., Berg, C.W., Nielsen, A., et al. 2017. glmmTMB balances speed and flexibility among packages for zero-inflated generalized linear mixed modeling. R J. **9**(2): 378. doi:10.32614/RJ-2017-066.

Brown, A.D., Sisneros, J.A., Jurasin, T., Nguyen, C., and Coffin, A.B. 2013. Differences in lateral line morphology between hatchery- and wild-origin steelhead. PLoS One, **8**(3): e59162. doi:10.1371/journal.pone.0059162.

Bunaciu, A.A., Udriştioiu, E.G., and Aboul-Enein, H.Y. 2015. X-ray diffraction: instrumentation and applications. Crit. Rev. Anal. Chem. **45**(4): 289–299. doi:10.1080/10408347.2014.949616.

Campana, S.E. 1999. Chemistry and composition of fish otoliths: pathways, mechanisms and applications. Mar. Ecol. Prog. Ser. **188**: 263–297. doi:10.3354/meps188263.

Delaval, A., Solås, M.R., Skoglund, H., and Salvanes, A.G.V. 2021. Does vaterite otolith deformation affect post-release survival and predation susceptibility of hatchery-reared juvenile Atlantic salmon? Front. Vet. Sci. **8**: 709850. doi:10.3389/fvets.2021.709850.

Doubleday, Z.A., Izzo, C., Woodcock, S.H., and Gillanders, B.M. 2013. Relative contribution of water and diet to otolith chemistry in freshwater fish. Aquat. Biol. **18**(3): 271–280. doi:10.3354/ab00511.

Dunmall, K.M., Langan, J.A., Cunningham, C.J., Reist, J.D., and Melling, H., Aklavik Hunters and Trappers Committee, Olokhaktomiut Hunters and Trappers Committee, Paulatuk Hunters and Trappers Committee, Sachs Harbour Hunters and Trappers Committee, Tuktoyaktuk Hunters and Trappers Committee, & Kugluktuk Hunters and Trappers Organization. 2024. Pacific salmon in the Canadian Arctic highlight a range-expansion pathway for sub-Arctic fishes. Global Change Biol. **30**(6): e17353. doi:10.1111/gcb.17353.

Dunmall, K.M., Bean, C.W., Berntsen, H.H., Ensing, D., Erkinaro, J., Irvine, J.R., et al. 2025. Invading and range-expanding Pink Salmon inform management actions for marine species on the move. ICES J. Mar. Sci. **82**(1): fsae199. doi:10.1093/icesjms/fsae199.

Erkinaro, J., Orell, P., Kytökorpi, M., Pohjola, J., and Power, M. 2023. Active feeding of downstream migrating juvenile Pink Salmon (*Oncorhynchus gorbuscha*) revealed in a large Barents Sea River using diet

and stable isotope analysis. J. Fish Biol. jfb.15625. doi:10.1111/jfb.15625.

Forsgren, E., Bærum, K.M., Finstad, A.G., Gjelland, K.Ø., Hesthagen, T., Knutsen, H., and og Wienerroither, R. 2023. Actinopterygii: Vurdering av pukkellaks Oncorhynchus gorbuscha for Fastlands-Norge med havområder. Fremmedartslista 2023. Artsdatabanken. Available from https://lister.artsdatabanken.no/fremmedartslista/2023/1909 [accessed 5 May 2026].

Gaffney, L., Polard, E., Kraemer, C., Walton, L., Covernton, G., Duguid, W., et al. 2026. Timing matters: early enrichment reduces vateritic otolith deformities in hatchery-reared coho salmon. Aquaculture, **620**: 743915. doi:10.1016/j.aquaculture.2026.743915.

Gaffney, L.P., Quindazzi, M., Polard, E., Kraemer, C., Walton, L.N., Molder, Z.A., et al. 2025. Vateritic otoliths in hatchery-reared Strait of Georgia coho salmon: variation among stocks, hatcheries, and life stages. Fish Res. **283**: 107296. doi:10.1016/j.fishres.2025.107296.

Gauldie, R.W. 1985. Vaterite otoliths from Chinook salmon (*Oncorhynchus tshawytscha*). NZ J. Mar. Freshwater Res. **20**(2): 209–217. doi:10.1080/00288330.1986.9516145.

Gjedrem, T., and Gunnes, K. 1978. Comparison of growth rate in Atlantic salmon, Pink Salmon, Arctic char, sea trout and rainbow trout under Norwegian farming conditions. Aquaculture, **13**(2): 135–141. doi:10.1016/0044-8486(78)90107-2.

Gordeeva, N.V., and Salmenkova, E.A. 2011. Experimental microevolution: transplantation of Pink Salmon into the European North. Evol. Ecol. **25**(3): 657–679. doi:10.1007/s10682-011-9466-x.

Hartig, F. 2024. DHARMa: residual diagnostics for hierarchical (multi-level/mixed) regression models. (Version 0.4.7) [R package]. Available from https://CRAN.R-project.org/package=DHARMa.

Heard, W. 1991. Life history of Pink Salmon (*Oncorhynchus gorbuscha*). I *In* C. Groot and L. Margolis (Editors)(Editors) Pacific salmon life histories. UBC Press, Vancouver(121–123).

ICES. 2022. Distribution and abundance of Pink Salmon across the North Atlantic. *In* Report of the ICES Advisory Committee, 2022. ICES Advice 2022, sal.oth.pink. International Council for the Exploration of the Sea. doi:10.17895/ices.advice.21020050.

Jensen, J., Christensen, G., Henriksen, E.H., Isaksen, O., Haugen, T.O., Thorkildsen, T.B., and Merkel, B. 2024. The Arctic queen and the Pacific invader: salmonid migrations in Svalbard. Fram Forum, **13**: 82–85. Available from https://framforum.com/2024/03/05/the-arctic-queen-and-the-pacific-invader-salmonidmigrations-in-svalbard/ [accessed 6 April 2025].

Kaev, A.M., Romasenko, L.V., and Kaev, D.A. 2023. Scale-based study of linear growth rate of Pink Salmon *Oncorhynchus gorbuscha* (Salmonidae). J. Ichthyol. **63**(1): 79–89. doi:10.1134/S0032945223010058.

Lennox, R.J., Berntsen, H.H., Garseth, Å.H., Hinch, S.G., Hindar, K., Ugedal, O., et al. 2023. Prospects for the future of Pink Salmon in three oceans: from the native Pacific to the novel Arctic and Atlantic. Fish Fish. faf.12760. doi:10.1111/faf.12760.

Lewis, L.S., Huang, J.L., Willmes, M., Fichman, R.A., Hung, T.-C., Ellison, L.T., et al. 2022. Visual, spectral, and microchemical quantification of crystalline anomalies in otoliths of wild and cultured delta smelt. Sci. Rep. **12**(1): 20751. doi:10.1038/s41598-022-22813-w.

Libungan, L.A., and Pálsson, S. 2015. ShapeR: an R package to study otolith shape variation among fish populations. PLoS One, **10**(3): e0121102. doi:10.1371/journal.pone.0121102.

Massicotte, P., and South, A. 2023. Rnaturalearth: World map data from natural earth. (Version 1.0.1) [R package]. Available from https://CRAN.R-project.org/package=rnaturalearth.

May, S.A., Shedd, K.R., Rand, P.S., and Westley, P.A.H. 2023. Tidal gradients, fine-scale homing and a potential cryptic ecotype of wild spawning Pink Salmon (*Oncorhynchus gorbuscha*). Mol. Ecol. mec.17154. doi:10.1111/mec.17154.

McConnell, C.J., Atkinson, S., Oxman, D., and Westley, P.A.H. 2019. Is blood cortisol or vateritic otolith composition associated with natal dispersal or reproductive performance on the spawning grounds of straying and homing hatchery-produced chum salmon (*Oncorhynchus keta*) in Southeast Alaska? Biol. Open, **8**(6): bio042853. doi:10.1242/bio.042853.

Mortensen, D.G., Wertheimer, A.C., Maselko, J.M., and Taylor, S.G. 2002. Survival and straying of Auke Creek, Alaska, Pink Salmon marked with coded wire tags and thermally induced otolith marks. Trans. Am. Fish. Soc. **131**(1): 14–26. doi:10.1577/1548-8659(2002)131⟨0014:SASOAC⟩2.0.CO;2.

Nielsen, J., Nygaard, R., Brandner, M., and Præbel, K. 2024. Occurrence of the invasive Pink Salmon (*Oncorhynchus gorbuscha*, Walbaum 1792) in Greenland 2020 and 2021 as revealed using citizen science, snorkeling, and environmental DNA metabarcoding of fishes in the Kapisillit River. Arct. Sci. **10**(3): 511–519. doi:10.1139/as-2023-0068.

Oxman, D.S., Barnett-Johnson, R., Smith, M.E., Coffin, A., Miller, D.L., Josephson, R., and Popper, A.N. 2007. The effect of vaterite deposition on sound reception, ototlith morphology, and inner ear sensory epithelia in hatchery-reared chinook salmon (*Oncorhynchus tshawytscha*). Can. J. Fish. Aquat Sci. **64**(11): 1469–1478. doi:10.1139/f07-106.

Paulsen, T., Sandlund, O.T., Østborg, G., Thorstad, E.B., Fiske, P., Muladal, R., and Tronstad, S. 2022. Growth of invasive Pink Salmon (*Oncorhynchus gorbuscha*) at sea assessed by scale analysis. J. Fish. Biol. **100**(1): 218–228. doi:10.1111/jfb.14937.

Payan, P., De Pontual, H., Edeyer, A., Borelli, G., Boeuf, G., and Mayer-Gostan, N. 2004. Effects of stress on plasma homeostasis, endolymph chemistry, and check formation during otolith growth in rainbow trout (*Oncorhynchus mykiss*). Can. J. Fish. Aquat. Sci. **61**: 1247–1255. doi:10.1139/f04-059.

Peck, T.P. 1970. Differentiation of hatchery and stream juvenile Coho salmon (*Oncorhynchus kisutch*) from Washington and Oregon by the use of scales and otoliths. Master's thesis, University of Washington.

Putman, N.F., Jenkins, E.S., Michielsens, C.G.J., and Noakes, D.L.G. 2014. Geomagnetic imprinting predicts spatio-temporal variation in homing migration of pink and sockeye salmon. J. R. Soc. Interface, **11**(99): 20140542. doi:10.1098/rsif.2014.0542.

Quinn, T.P. 1993. A review of homing and straying of wild and hatchery-produced salmon. Fish Res. **18**(1): 29–44. doi:10.1016/0165-7836(93)90038-9.

Quinn, T.P. 2018. The behavior and ecology of Pacific salmon and trout. University of Washington Press.

R Core Team. 2025. R: a language and environment for statistical computing. Available from http://www.r-project.org/.

Reimer, T., Dempster, T., Warren-Myers, F., Jensen, A.J., and Swearer, S.E. 2016. High prevalence of vaterite in sagittal otoliths causes hearing impairment in farmed fish. Sci. Rep. **6**(April): 25249. doi:10.1038/srep25249.

Reimer, T., Dempster, T., Wargelius, A., Fjelldal, P.G., Hansen, T., Glover, K.A., et al. 2017. Rapid growth causes abnormal vaterite formation in farmed fish otoliths. J. Exp. Biol. **220**(16): 2965–2969. doi:10.1242/jeb.148056.

Ruggerone, G., Springer, A., Van Vliet, G., Connors, B., Irvine, J., Shaul, L., et al. 2023. From diatoms to killer whales: impacts of Pink Salmon on North Pacific ecosystems. Mar. Ecol. Prog. Ser. **719**: 1–40. doi:10.3354/meps14402.

Sandlund, O.T., Berntsen, H.H., Fiske, P., Kuusela, J., Muladal, R., Niemelä, E., et al. 2019. Pink salmon in Norway: the reluctant invader. Biol. Invasions, **21**(4): 1033–1054. doi:10.1007/s10530-018-1904-z.

Sharp, D., Sharr, S., and Peckahm, C. 1994. Homing and straying patterns of coded wire tagged Pink Salmon in Prince William Sound. *In* B. Smoker(Editor), Proceedings of the 16th Northeast Pacific pink & chum salmon workshop. Alaska Sea Grant College Report No 94-02. pp. 77–82.

Simmons, O.M., Paulsen, T., Berntsen, H.H., Diserud, O., Fiske, P., Østborg, G., et al. 2026. Early marine growth and spawning body size vary by year and region in invasive Pink Salmon (*Oncorhynchus gorbuscha*). Aquat. Sci. **88**: 77. doi:10.1007/s00027-026-01309-z.

Skóra, M.E., Jones, J.I., Youngson, A.F., Robertson, S., Wells, A., Lauridsen, R.B., and Copp, G.H. 2023. Evidence of potential establishment of Pink Salmon *Oncorhynchus gorbuscha* in Scotland. J. Fish. Biol. **102**(3): 721–726. doi:10.1111/jfb.15304.

Skóra, M.E., Guðbergsson, G., Copp, G.H., and Jones, J.I. 2024. Evidence of successful recruitment of non-native Pink Salmon *oncorhynchus gorbuscha* in Iceland. J. Fish. Biol. **104**(1): 329–334. doi:10.1111/jfb.15556.

Staveley, T.A.B., Bergendahl, I.A., Bárðarson, H., Berntsen, H.H., Eliasen, K., Erkinaro, J., et al. 2025. Status and future perspectives of Pink Salmon in the Nordic region. Boreal Environ. Res. **30**: 149–162.

Strong, M.B., Neilson, J.D., and Hunt, J.J. 1986. Aberrant crystallization of pollock (*Pollachius virens*) otoliths. Can. J. Fish. Aquat. Sci. **43**(7): 1457–1463. doi:10.1139/f86-180.

Sweeting, R.M., Beamish, R.J., Noakes, D.J., and Neville, C.M. 2003. Replacement of wild Coho salmon by hatchery-reared Coho salmon in the Strait of Georgia over the past three decades. North Am. J. Fish. Manage. **23**(2): 492–502. doi:10.1577/1548-8675(2003)023%3C0492:ROWCSB%3E2.0.CO;2.

Sweeting, R.M., Beamish, R.J., and Neville, C.M. 2004. Crystalline otoliths in teleosts: comparisons between hatchery and wild Coho salmon (*Oncorhynchus kisutch*) in the Strait of Georgia. Rev. Fish Biol. Fish. **14**: 361–369. doi:10.1007/s11160-005-3793-3.

Tarpey, C.M., Seeb, J.E., McKinney, G.J., Templin, W.D., Bugaev, A., Sato, S., and Seeb, L.W. 2018. Single-nucleotide polymorphism data describe contemporary population structure and diversity in allochronic lineages of Pink Salmon (*Oncorhynchus gorbuscha*). Can. J. Fish. Aquat. Sci. **75**(6): 987–997. doi:10.1139/cjfas-2017-0023.

Thedinga, J.F., Wertheimer, A.C., Heintz, R.A., Maselko, J.M., and Rice, S.D. 2000. Effects of stock, coded-wire tagging, and transplant on straying of Pink Salmon (*Oncorhynchus gorbuscha*) in southeastern Alaska. Can. J. Fish. Aquat. Sci. **57**(10): 2076–2085. doi:10.1139/f00-163.

Thomas, O.R.B., Swearer, S.E., Kapp, E.A., Peng, P., Tonkin-Hill, G.Q., Papenfuss, A., et al. 2019. The inner ear proteome of fish. FEBS J. **286**(1): 66–81. doi:10.1111/febs.14715.

Thorstad, E., Staveley, T.A.B., and Fiske, P. 2024. Pink salmon in rivers: current knowledge, overlap and potential interactions with Atlantic salmon (Report No. CNL(24)51). North Atlantic Salmon Conservation Organization (NASCO).

Thorstad, E., Frøiland, E., Fagard, P., Kvaal, M., Lehne, C., Liberg, E., et al. 2025. Assessing the extraordinary measures used to counteract invasion of Pink Salmon into the North Atlantic. Manage. Biol. Invasions, 465–487. doi:10.3391/mbi.2025.16.2.09.

Tomás, J., and Geffen, A.J. 2003. Morphometry and composition of aragonite and vaterite otoliths of deformed laboratory reared juvenile herring from two populations. J. Fish. Biol. **63**(6): 1383–1401. doi:10.1111/j.1095-8649.2003.00245.x.

Tzeng, W.N., Chang, C.W., Wang, C.H., Shiao, J.C., Iizuka, Y., Yang, Y.J., et al. 2007. Misidentification of the migratory history of anguillid eels by Sr/Ca ratios of vaterite otoliths. Mar. Ecol. Prog. Ser. **348**: 285–295. doi:10.3354/meps07022.

Vignon, M., and Aymes, J.-C. 2020. Functional effect of vaterite—the presence of an alternative crystalline structure in otoliths alters escape kinematics of the brown trout. J. Exp. Biol. **223**(12): jeb222034. doi:10.1242/jeb.222034.

VKM. 2020. Assessment of the risk to Norwegian biodiversity and aquaculture from Pink Salmon (*Oncorhynchus gorbuscha*). Scientific Opinion of the Panel on Alien Organisms and Trade in Endangered Species (CITES). VKM report 2020:01, ISBN: 978-82-8259-334-2, ISSN: 2535-4019. Norwegian Scientific Committee for Food and Environment (VKM), Oslo, Norway.

Volk, E.C., Schroder, S.L., and Grimm, J.J. 1999. Otolith thermal marking. Fish Res. **43**(1–3): 205–219. doi:10.1016/S0165-7836(99)00073-9.

Weller, H. 2019. Countcolors: locates and counts pixels within color range(s) in images. (Version 0.9.1) [R package]. Available from https://CRAN.R-project.org/package=countcolors.

Wickham, H. 2009. ggplot2: elegant graphics for data analysis. Springer Science & Business Media. doi:10.1007/978-0-387-98141-3.

Wood, R.S., Chakoumakos, B.C., Fortner, A.M., Gillies-Rector, K., Frontzek, M.D., Ivanov, I.N., et al. 2022. Quantifying fish otolith mineralogy for trace-element chemistry studies. Sci. Rep. **12**: 2727. doi:10.1038/s41598-022-06721-7.

Appendix A

Two alternative models applying a 10% and 33% vaterite threshold was evaluated because the original all–or–nothing approach (0% threshold) may oversimplify the true condition of the sampled stocks. A key limitation is the lack of published literature defining the level at which vaterite begins to negatively affect fish performance. Consequently, classifying otoliths as vateritic based solely on the presence of any vaterite may potentially misrepresent stock–level effects. However, applying 10% or 33% threshold did not yield substantially different results compared to the all–or–nothing approach. As shown in Table A4, the primary difference is that the zero–inflated component shifts from being statistically significant under the 0% threshold to non–significant when the 10% threshold is applied.

Despite this statistical difference, the biological relevance of this shift is difficult to assess. Currently, the open literature does not define a biologically meaningful vaterite cutoff, and vaterite is generally treated using a presence/absence (0%) criterion, either explicitly or implicitly. To maintain comparability with previous studies and given the absence of empirical evidence supporting an alternative threshold, we therefore adopted the 0% cutoff in the main analyses. While it is possible that some studies apply informal thresholds without explicitly stating them, there is no consensus on when vaterite coverage begins to impair fish performance.

Table A1. The table shows results from the original gv_2 model and from two alternative models in which otoliths with <10% and <33% vaterite were classified as aragonitic.

	0% cutoff (gv_2)	10% cutoff	33% cutoff
	Conditional component		
Atlantic (intercept)	0.521	0.587	0.689
Pacific hatchery	**0.576**	**0.635**	**0.736**
Pacific wild	0.532	0.554	0.650
	Zero-inflated component		
Atlantic (intercept)	0.098	0.175	0.385
Pacific hatchery	**0.171**	0.232	0.378
Pacific wild	0.111	0.136	0.340

Note: Bold values indicate statistical significance at $p < 0.05$. Model estimates expressed as proportions. Conditional component represents the mean vaterite coverage when vaterite is present, while the zero-inflated component represents the proportion of samples with no vaterite.

Table A2. Measuring conditions applied during X-ray diffraction analysis using a Bruker D8 A25 DaVinci instrument for the identification and quantification of calcium carbonate mineral phases in otolith samples.

Radiation	CuKα (1.54 Å)
Detector	LynxEye^{TM} SuperSpeed
Monochromator	No
Generator	40 kV, 40 mA
Divergence slit	Variable, 6 mm
Scanning range	20°–80° 2θ
Step size	0.013° 2θ
Measuring time	1.145 s/step

Table A3. Morphological measurements of juvenile otoliths.

	Left			Right		
	Min	Mean	Max	Min	Mean	Max
Otolith area (mm^2)	0.0772	**0.1428**	0.2148	0.0886	**0.1445**	0.2370
Otolith width (mm)	0.2865	**0.3774**	0.4676	0.3004	**0.3771**	0.4991
Otolith length (mm)	0.3492	**0.4767**	0.6068	0.3672	**0.4856**	0.6446
Otolith perimeter (mm)	1.0144	**1.3778**	1.6832	1.0823	**1.3883**	1.7849

Note: Minimum and maximum measurements include all data points, including instances where only one otolith of the pair is present. Mean measurements are calculated exclusively from pairs where both otoliths are intact.

Table A4. Statistical results of a linear model analyzing the relationship between visually assessed vaterite coverage and XRD-derived vaterite coverage.

Parameter	Estimate	SE	*t*-value	*p*-value	Residual SE	R^2
Intercept	0.02619	0.01633	1.604	0.128		
Vaterite—XRD	0.95930	0.02665	35.992	<0.001	0.03566	0.9870

Fig. A1. Residuals (*a*) and residuals versus fitted (*b*) for linear model of method validation.

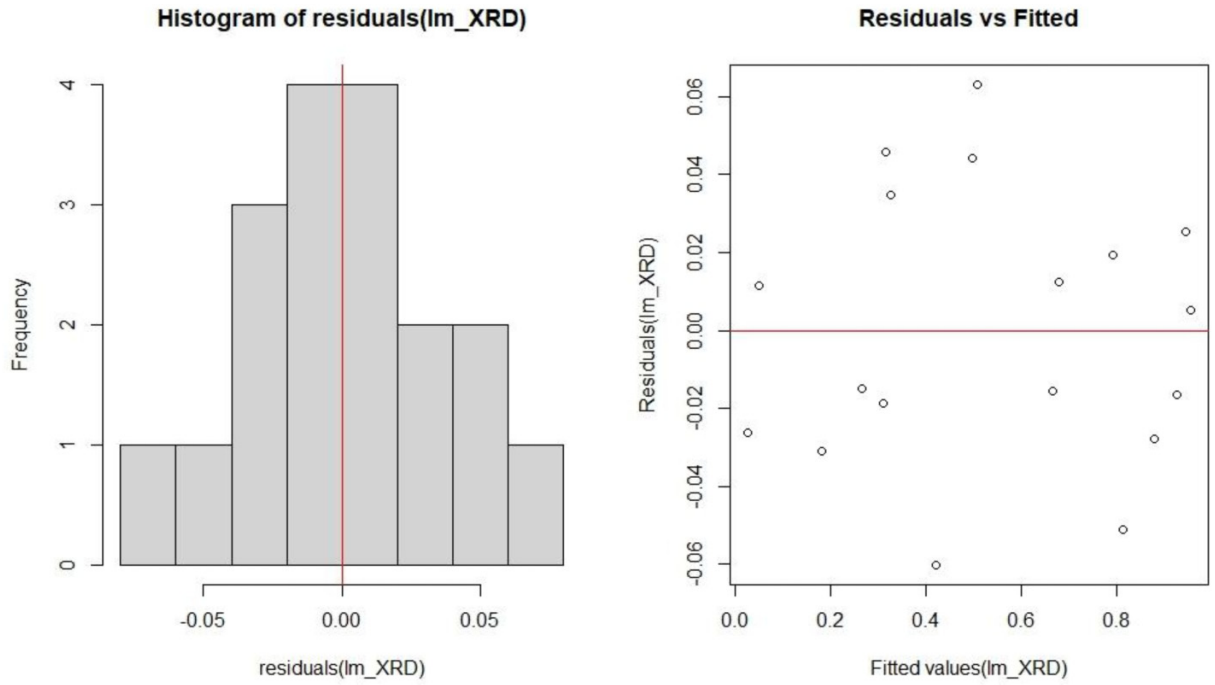

Fig. A2. Diagnostic plot for gv_3 using the DHARMa diagnostic plot.

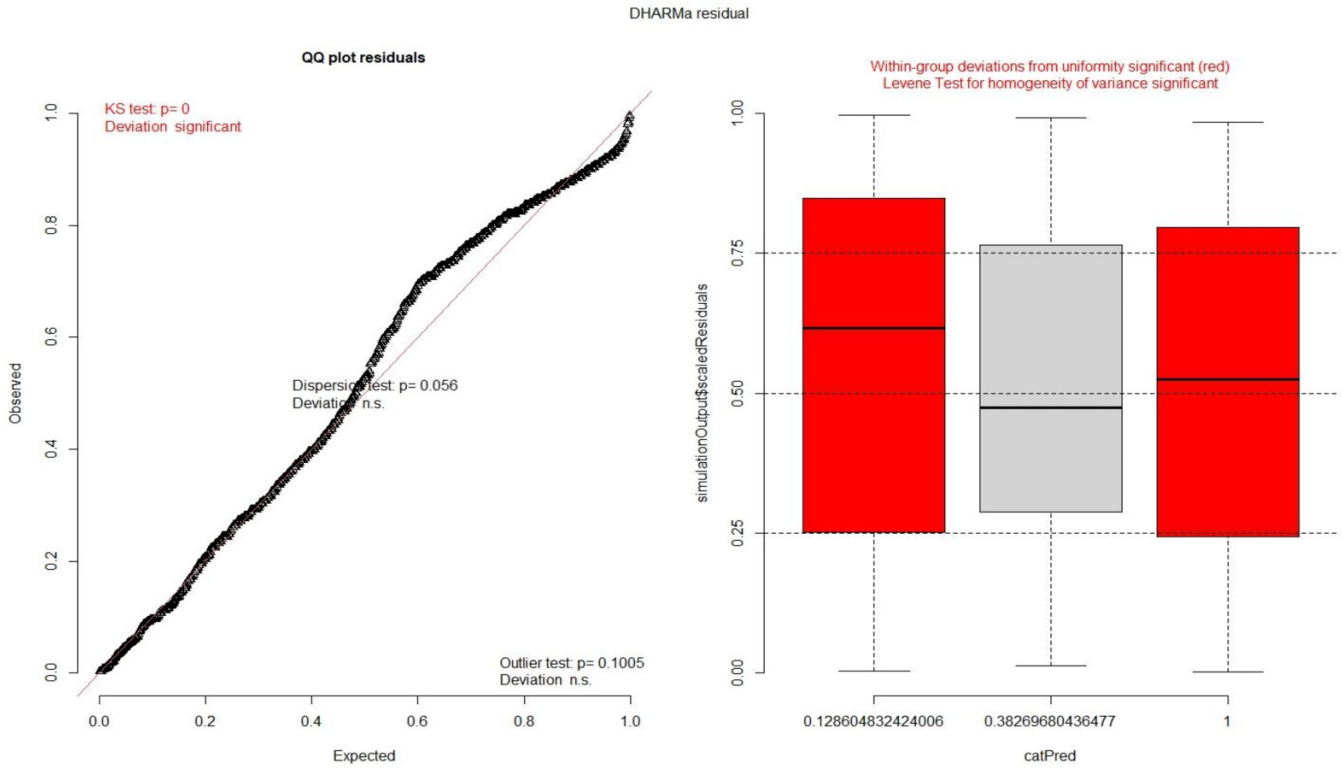

Fig. A3. (*a*) Juvenile Pink Salmon (30–40 mm). (*b*) Juvenile otolith showing no sign of vaterite development. (*c*) Juvenile otolith showing sign of vaterite on the right side of the otolith.

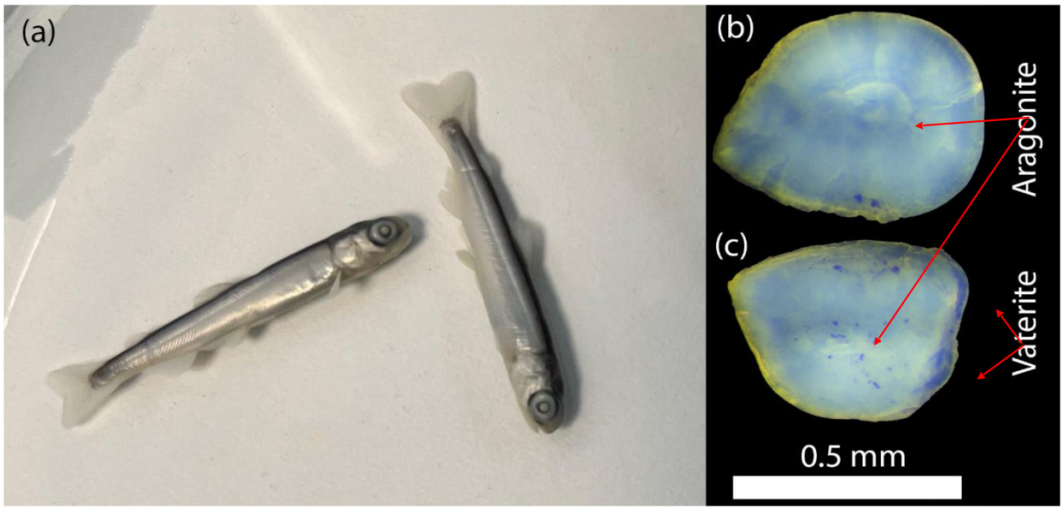
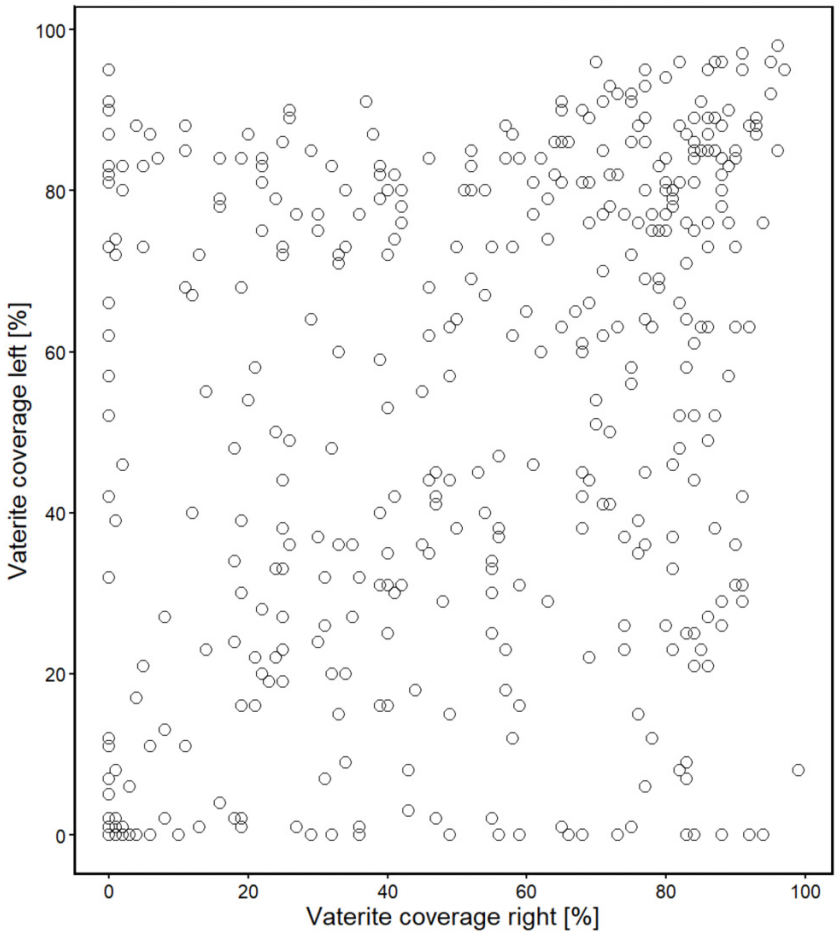
Fig. A4. Scatterplot illustrating the relationship in vaterite coverage between left and right otoliths from the same individuals. The random distribution of points suggests that vaterite formation occurs independently in each otolith. If a systematic difference in vaterite coverage existed between the left and right otoliths, we would expect a higher density of points in either the upper left or lower right corner of the plot.